NANO LETTERS

xxxx
Vol. 0, No. 0
A−G

Mechanisms of 1D Crystal Growth in Reactive Vapor Transport: Indium Nitride Nanowires

Sreeram Vaddiraju,[†] Aditya Mohite,[‡] Alan Chin,[||] M. Meyyappan,[||] Gamini Sumanasekera,[§] Bruce W. Alphenaar,[‡] and Mahendra K. Sunkara*,[†]

Departments of Chemical Engineering, Electrical and Computer Engineering, and Physics, University of Louisville, Louisville, Kentucky 40292, and Center for Nanotechnology, NASA Ames Research Center, Moffett Filed, California 94035

Received March 24, 2005; Revised Manuscript Received June 15, 2005

ABSTRACT

Indium nitride (InN) nanowire synthesis using indium (In) vapor transport in a dissociated ammonia environment (reactive vapor transport) is studied in detail to understand the nucleation and growth mechanisms involved with the so-called "self-catalysis" schemes. The results show that the nucleation of InN crystal occurs first on the substrate. Later, In droplets are formed on top of the InN crystals because of selective wetting of In onto InN crystals. Further growth via liquid-phase epitaxy through In droplets leads the growth in one dimension (1D), resulting in the formation of InN nanowires. The details about the nucleation and growth aspects within these self-catalysis schemes are rationalized further by demonstrating the growth of heteroepitaxially oriented nanowire arrays on single-crystal substrates and "tree-like" morphologies on a variety of substrates. However, the direct nitridation of In droplets using dissociated ammonia results in the spontaneous nucleation and basal growth of nanowires directly from the In melt surface, which is quite different from the above-mentioned nucleation mechanism with the reactive vapor transport case. The InN nanowires exhibit a band gap of 0.8 eV, whereas the mixed phase of InN and In_2O_3 nanowires exhibit a peak at ~1.9 eV in addition to that at 0.8 eV.

The synthesis of one-dimensional (1D), group-III-nitride nanostructures such as indium nitride (InN), gallium nitride (GaN), and aluminum nitride (AlN), has been accomplished mainly by using catalyst-assisted or oxide-assisted growth methods.[1−4] In the case of catalyst-metal-cluster-assisted techniques, gold clusters have served mostly as templates for the 1D growth of III-nitrides.[1−3] In the case of oxygen-assisted techniques, oxide sheaths around crystals assisted the growth of III-nitrides in one dimension.[4] A completely different concept, involving the use of low-melting metal mediums for the multiple nucleation and growth of nanowires, was also reported in the literature.[5−8] The solubility of nitrogen in low-melting metals including Group III metals (Ga, In, Al) is extremely low. Therefore, the dissolution of nitrogen into low-melting metals is expected to yield crust formation or multiple nanowire growth from molten metal pools.[6] This phenomenon should be true even when low-melting metal droplets become smaller.[9] An alternative is to use the vapor transport of In onto substrates in the presence of decomposed ammonia in a reactive vapor transport approach.[10−13] Recent studies have shown that the combined vapor transport of indium (In) and decomposed ammonia onto substrates leads to the formation of 1D InN structures.[10] This nanowire synthesis method is henceforth referred to as "reactive vapor transport" in this manuscript. However, the nucleation and growth mechanisms leading to the formation of 1D structures in reactive vapor transport methods are not understood. Knowledge on the nucleation and early stages of growth could potentially lead to control over the size and the growth direction of the resulting nanowires. Concisely, the main questions are the following: (1) What is the nucleation mechanism that explains nanowire formation in reactive vapor transport experiments? (2) Why does the growth occur in one dimension?

Synthesis of heteroepitaxial nanowire arrays on single-crystal substrates is important for the integration of nanowires into device applications. Similarly, rational approaches for synthesizing highly branched nanowire systems (tree-like structures) could be important for increasing the area for interfacial processes in applications such as catalysis and energy conversion. Thus far, only catalyst-metal-assisted techniques have been shown to produce heteroepitaxially oriented arrays of nanowires.[14] In addition, the synthesis of branched nanowires resembling a "tree formation" has been reported recently with the continuous use of catalytic metal

* Corresponding author. Tel: 502-852-1558; fax: 502-852-6355; e-mail: mahendra@louisville.edu.
[†] Department of Chemical Engineering.
[‡] Department of Electrical and Computer Engineering.
[§] Department of Physics.
[||] NASA Ames Research Center.

10.1021/nl0505804 CCC: $30.25
Published on Web 00/00/0000

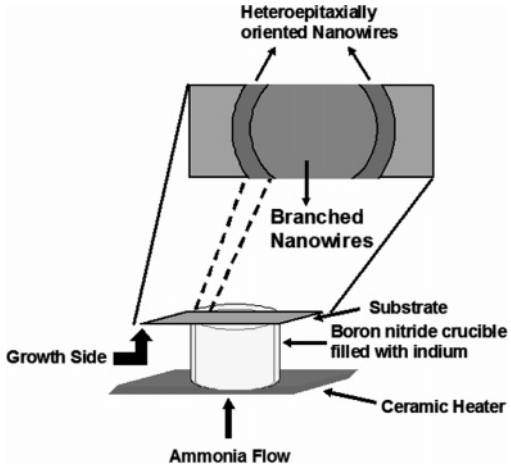

Figure 1. Schematic representation of the experimental setup used for the reactive vapor transport experiments. The regions on the substrates where branched and heteroepitaxially oriented nanowires are obtained are marked on the figure.

clusters.[15] Hence, the question is whether direct synthesis techniques such as reactive vapor transport can be employed in synthesizing heteroepitaxially oriented nanowire arrays and branched nanowires. This can only be understood and rationalized with knowledge on the nucleation and initial stages of growth leading to nanowire formation in direct synthesis schemes. Direct synthesis approaches are highly desirable because the presence of the catalyst metal in the indirect schemes may pose processing issues during device fabrication.

In this regard, this paper is aimed at understanding the nucleation and growth mechanism responsible for 1D crystal growth in these reactive vapor transport schemes. InN nanowire synthesis is used here as a case study because of the interest in III-nitrides for various optoelectronics and high-temperature electronics applications. In addition, InN has been the subject of renewed interest because of its recently reported band gap of 0.8 eV measured at room temperature,[10,16] as opposed to the band gap of 1.9 eV assumed previously.[17] Most of the explanations provided in the literature for the peak observed at 1.9 eV are centered on the presence of oxygen in the synthesized InN.[18] It is critical to establish the band gap and understand the origin of the alternate peaks reported previously in order to realize many potential applications of InN.

Reactive vapor transport experiments for the synthesis of InN nanowires were performed in a vacuum chamber equipped with all of the necessary accessories such as pressure transducers for pressure measurement and thermocouples for substrate temperature measurement. A schematic representation of the setup used for the experiments is shown in Figure 1. The setup consists of a boron nitride crucible filled with In, placed on top of a ceramic heater (GE Advanced Ceramics). The substrates used for the nanowire synthesis were mounted on top of the boron nitride crucible, partially covering it. Prior to each experimental run, the In was cleaned using a 10 vol % nitric acid solution, followed by cleaning with distilled water and acetone to remove any native oxide layer present on the surface. The cleaning of

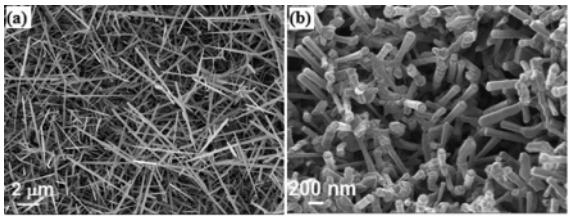

Figure 2. Scanning electron micrographs of InN nanowires synthesized at a substrate temperature of 450 °C on (a) amorphous quartz substrates and (b) polycrystalline AlN substrates. The presence of crystals at the tip of the nanowires can be observed clearly in the micrograph.

the native oxide layer on the as-received In source was observed to be a crucial step in preventing the formation of any undesired indium oxide phase in the samples. The vapor transport experiments were performed using 140 sccm of ammonia at a total reactor pressure of 250 mTorr. The substrate heater was maintained at various temperatures ranging from 650 to 850 °C. The corresponding substrate temperatures ranged from 400 to 480 °C. Various substrates including amorphous quartz, polycrystalline aluminum nitride (AlN), polycrystalline gallium nitride (GaN), R-plane oriented sapphire, highly oriented pyrolytic graphite (HOPG), and pyrolytic boron nitride (pBN) were used for the synthesis experiments. The growth time was typically 60 min and the samples were characterized extensively for morphology, phase, and growth direction using scanning electron microscopy (SEM), X-ray diffraction (XRD), and transmission electron microscopy (TEM), respectively.

The band gap of InN nanowires was determined using two different techniques, photogenerated displacement current measurements and scanning tunneling spectroscopy (STS) in an ultrahigh vacuum (UHV) environment. The first technique uses photogenerated displacement current measurements of the samples as described in detail elsewhere.[19] Briefly, the procedure is as follows: the as-synthesized samples were mounted on a copper block and a contact to the nanowires was made using silver ink. In this configuration, the setup works like a metal-insulator-semiconductor (MIS) capacitor with InN nanowires being the semiconductor material. A pulsed optical parametric amplifier (OPA) (Spectra Physics, California) excitation source, whose output is tunable between 0.4 and 4 eV, was used for these measurements. STS characterization of the samples was performed using a UHV scanning tunneling microscope (STM) (RHK Technologies, Michigan).

Reactive vapor transport experiments using a heater temperature (for In vaporization and ammonia decomposition) of 750 °C and a substrate temperature of 450 °C resulted in InN nanowires as shown in Figure 2. The nanowires obtained on both quartz (Figure 2a) and polycrystalline AlN (Figure 2b) substrates are straight and approximately 100 nm in diameter and a few micrometers long. In both cases, the nanowires contained either well-faceted, 3D crystals at their tips or smooth-looking droplets. An extensive investigation using energy dispersive spectroscopy (EDS) X-ray mapping indicates that the nanowire tips contain mostly In and small amounts of N. An XRD pattern (see supporting

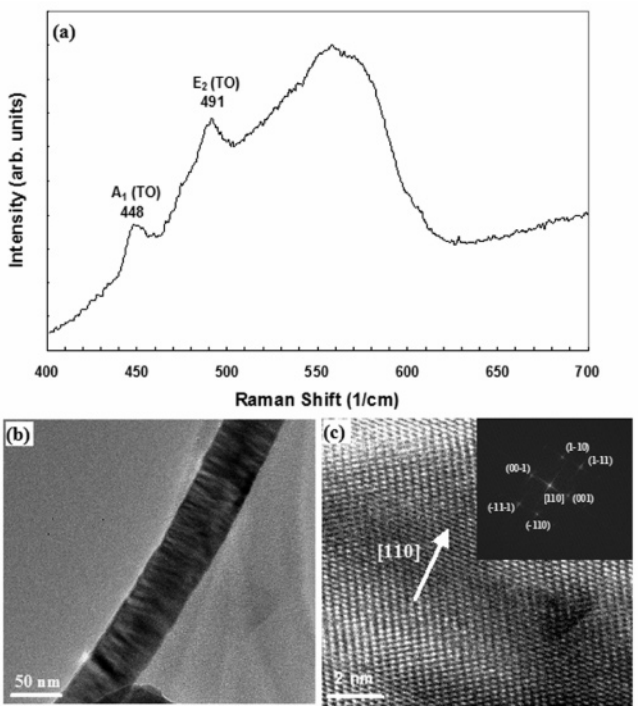

Figure 3. (a) Raman spectra of the synthesized InN nanowires, showing the primary peaks corresponding to wurtzite InN. (b) Low-magnification TEM image of an InN nanowire. (c) High-resolution micrograph of the wire showing no amorphous sheath around the nanowire. SAD pattern of the nanowire along the [110] zone axis is shown in the inset. The diffraction pattern indicates the growth direction of the nanowire to be [110].

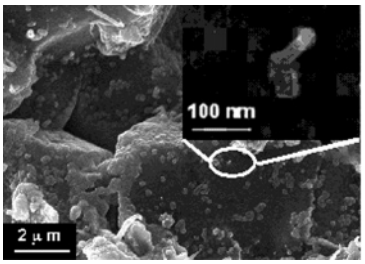

Figure 4. (a) Nuclei of InN observed on the polycrystalline AlN substrate after 10 min at a substrate temperature of 450 °C. The initial stages of growth of a nanowire from an InN crystal is shown clearly in the inset.

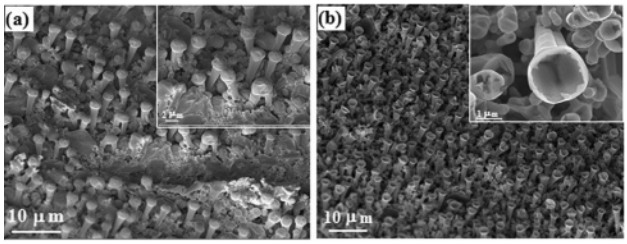

Figure 5. (a) Micrograph of InN nanowires synthesized on a HOPG substrate at 450 °C. The presence of In droplets is shown clearly in the high-magnification image shown in the inset. (b) Side view images of the oriented InN nanowires synthesized on HOPG substrates, after treatment in a 50 vol % sulfuric acid solution for 10 min. InN shells at the tips of the nanowires can be observed easily in the micrographs. The acid etching procedure employed removed excess In at the tips of the nanowires.

information) of the synthesized InN nanowires over a large area (∼1 square inch area) showed all of the primary reflections corresponding to InN. The Raman spectrum of the as-synthesized nanowires shows all peaks corresponding to wurtzite InN [20] and is presented in Figure 3a. Figure 3b is a low-magnification TEM micrograph of a straight InN nanowire. HR-TEM analysis of the nanowires (Figure 3c) indicates the growth direction of the nanowires to be [110]. The nanowires have no detectable amorphous sheath, and the selected area diffraction (SAD) pattern also confirms the growth direction of the nanowire to be [110]. (See inset of Figure 3c).

To understand the nucleation and growth mechanisms involved in the formation of these InN nanowires, we performed short-term experiments, spanning 10 min, using polycrystalline AlN substrates. Short-term experiments, after a 10-min run using a heater temperature of 750 °C and a substrate temperature of 450 °C, resulted in a high density of InN crystals as shown in Figure 4. The results also show In droplet-led 1D nanorods formed during the early stages (see inset in Figure 4). These results indicate that the InN crystal nucleation occurs first and then the In droplet-led growth of the underlying crystal occurs in one dimension for nanowires as shown in the inset to Figure 4a. This has not been reported in previous studies on the self-catalysis growth of nanowires. [21]

Further evidence of this tip-led growth comes from InN nanowire synthesis experiments performed using HOPG substrates, as shown in Figure 5a. In this case, almost all of the nanowires are oriented perpendicular to the substrate and they exhibited larger droplets at their tips (see inset in Figure 5a). EDS X-ray mapping of these samples does not indicate the presence of any other metal besides indium. To confirm that the tips are composed primarily of In, we cleaned the as-synthesized nanowires using 50 vol % sulfuric acid in water. Sulfuric acid reacts only with In metal and does not react with InN at a significant rate. The acid cleaning step selectively removed the indium at the tips of the nanowires. Micrographs of the InN nanowires after acid treatment are shown in Figure 5d. The presence of InN shells at the tips of the nanowires can be observed clearly in the micrographs. This confirms the presence of In metal droplets at the tips of the nanowires. The InN shells were observed at several of the nanowire tips after the acid dissolution of In. The observation of InN shells was more conspicuous on the larger droplets such as those shown in Figure 5b. The chances of InN crust formation increases with increasing In droplet size because the nanowire growth kinetics compete with the spontaneous nucleation of InN from In droplets. The formation of InN crust could limit further growth if it occurs during nanowire growth. But, the InN crust could have also formed during the shutdown of the experiment that has not been resolved with the present studies.

Short-term experiments were also performed at higher In vapor pressures by increasing the heater temperature to 850 °C (substrate temperature = 480 °C). The results show another distinct mode of nanowire growth as shown in Figure 6. The increased In vapor pressures resulted in high amounts

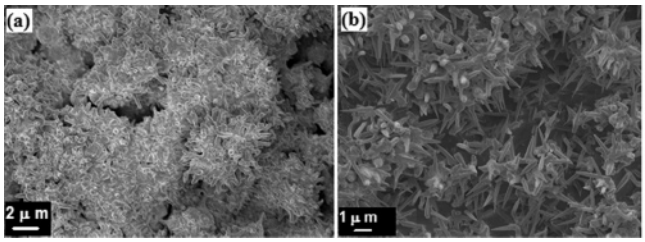

Figure 6. Multiple nucleation and growth of InN nanowires from In droplets observed at a higher substrate temperature of 480 °C after (a) 10 min and (b) 1 h.

of In condensation on the substrate in the initial stages. This led to the formation of several micrometer-sized In droplets with no InN crystal formation on the substrate in the initial stages. Further nitridation results, shown in Figure 6a, indicate the multiple nucleation and growth of InN nanowires from the several micrometer-sized In droplets, as expected from our previous studies. The average diameter of the synthesized nanowires was around 250 nm. Here, the increase in size was seen at the bottom of the nanowires indicating substantial basal growth. Longer duration experiments performed under the same conditions led to longer nanowires with In droplets at the tips, and the final wire morphologies looked similar to the results shown in Figure 6b.

The results from both short and longer duration experiments under low and high In vapor pressures indicate two distinct nucleation mechanisms during the reactive vapor transport technique for 1D crystal growth. The proposed nucleation and growth mechanisms are illustrated schematically in Figure 7. These two types of proposed mechanisms are explained in detail below.

In the first set of experiments (Case I) with lower In vapor, no In metal thin film was formed on the substrate in the initial stages (because of the low In vapor pressures at low heater temperatures). In this case, the saturation of the substrate surface with the incoming In and N atoms occurs first leading to the formation of a high density of small InN crystals. Subsequent In flux gets adsorbed either on the substrate surface or on the indium crystal nuclei. Because In preferentially wets InN rather than the substrate material, the In atoms adsorbed on the substrate migrate to the nearest InN crystal nuclei and from droplets on their surfaces. This selective wetting of In on InN can be inferred from earlier studies of Al on AlN.[22] The dissolution of nitrogen into the indium droplets on InN crystals led to the growth of InN in one dimension in the form of a nanowire. This tip-led growth of InN nanowires occurs primarily by a mechanism called "liquid-phase epitaxy" through In droplets onto underlying InN crystals. In summary, the nucleation and growth of InN nanowires is inferred to occur as follows: (a) formation of InN crystal nuclei because of the reaction between In vapor and N (from ammonia decomposition at the heater) transported onto the substrate; (b) formation of In droplets on the surface of the InN nuclei because of the selective wetting of InN by In molten metal in the presence of hydrogen and ammonia in the gas phase; and (c) selective growth into 1D nanowires through In droplets by liquid-phase epitaxy. This is represented schematically in Figure 7I.

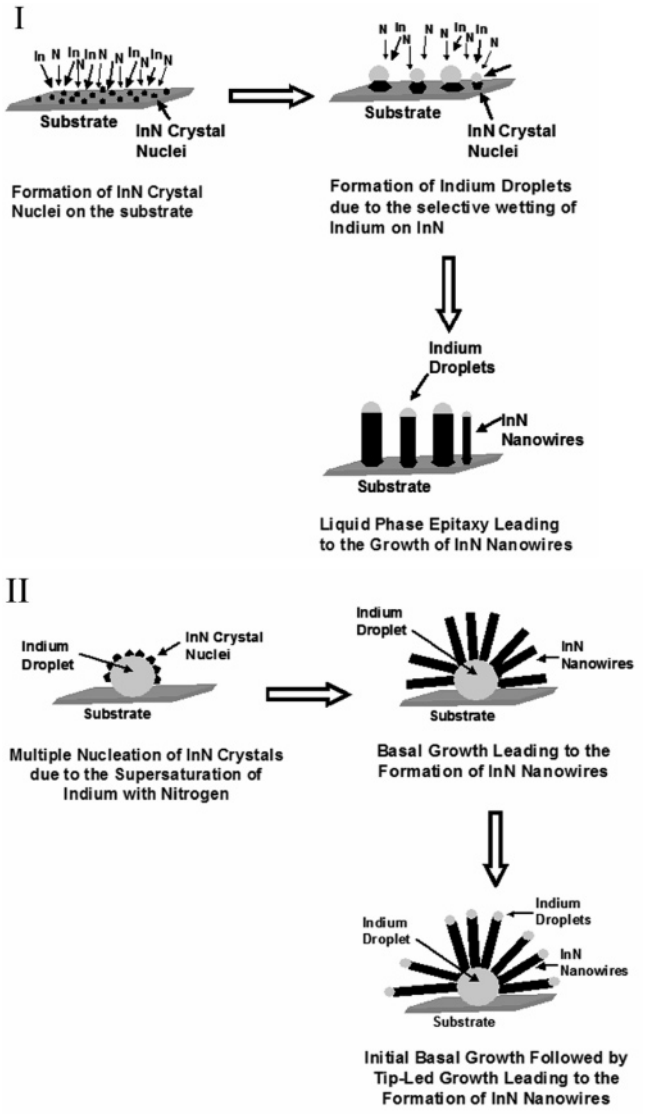

Figure 7. Schematic representation of the growth mechanism proposed for the growth of InN nanowires synthesized by the vapor transport of In in the presence of ammonia. (I) The formation of InN crystal nuclei, followed by the formation of In droplets on the crystal nuclei. The nitridation of the droplets leads to the 1D growth of InN nanowires by a tip-led growth route. (II) Multiple nucleation and growth of InN nanowires in a basal growth mode because of the supersaturation of In droplets with nitrogen dissolving from the gas phase.

In the second set of experiments (Case II), a high flux of In vapor resulted in the formation of large In droplets on the substrate during initial stages, without any InN crystals. Here, a higher flux of In vapor is supplied onto the substrates using higher heater temperatures. Atomic nitrogen (from decomposed ammonia) gets dissolved into these large In droplets. Because the solubility of nitrogen in In is small at the temperature used (480 °C), the direct nitridation and supersaturation of In droplets with nitrogen led to the multiple nucleation of InN crystals on the surface of In. The growth of these nuclei into nanowires can occur by either (i) basal growth or (ii) basal growth followed by growth with liquid-phase epitaxy through In droplets at the tips. This is represented schematically in detail in Figure 7II. In this case,

control over the diameter of the obtained nanowires could be accomplished by varying the degree of nitrogen supersaturation in the large In droplets, by varying the atomic nitrogen flux (or partial pressure), and by varying the substrate temperature. In addition, we believe that the growth direction of the nanowires is different in the two growth mechanisms. This can be inferred from our work on GaN nanowire synthesis.[23] For the case of GaN, it was observed that nanowires synthesized via reactive vapor transport (Case I) always have a <10−10> growth direction. In the second case, with direct nitridation of micrometer-sized Ga droplets, the nanowires synthesized during multiple nucleation and basal growth (case II) always have a ⟨0001⟩ growth direction.[23]

As stated earlier, the experiments involving low In vapor flux led to InN crystal formation in the initial stages. This fact alone allowed us to hypothesize that using the reactive vapor transport conditions could lead to InN heteroepitaxy with underlying substrates if single-crystal substrates were used. This hypothesis was tested using single-crystal R-plane-oriented sapphire substrates and hexagonal platelet-shaped, single crystals of GaN. Experiments using R-plane sapphire substrates and c-plane GaN crystals resulted in heteroepitaxially oriented InN nanowire arrays over large areas (5 mm × 10 mm). Representative images of heteroepitaxially oriented nanowires synthesized on an R-plane sapphire are shown in Figure 8a. These nanowires are tapered, and their diameters vary from 15 nm at the base to 100 nm at the tip. The thin parts of the nanowires close to the sapphire substrate are highlighted in Figure 8. Nanowires synthesized on GaN platelet-shaped crystals (Figure 8b) are tapered with sub-20-nm thicknesses at the GaN−InN interface and thickened toward the top. The nanowires are oriented randomly on the A-plane of the GaN platelets as highlighted in Figure 8b. A high-magnification image of InN nanowires oriented perpendicular to the C-plane of a GaN platelet are also shown in the inset in Figure 8b. These results suggest that the oriented growth of nanowires as small as 15 nm or even lower could be accomplished on single-crystal substrates. Here, the increase seen with In droplet sizes at the tips could have occurred because of the high amount of direct adsorption of In from the vapor as the geometric cross-sectional area of the substrate is dominated by the tips. It is entirely possible that the In atoms also diffuse to the top of the wire and join the In droplet because the diffusion length exceeds a few micrometers.[24]

In the case of excessive In condensation onto the growing nanowires, the formation of In droplets can also occur directly along the length of the growing nanowires specifically when they are oriented randomly on the substrate. Liquid-phase epitaxy on these additional In droplets condensing on the growing nanowires, in the absence of conditions leading to spontaneous nucleation, will lead to another set of nanowires from each nanowire. The same process can repeat itself on the new nanowire branches and lead to a tree-like formation. To test such phenomena, we conducted experiments using several substrates (quartz, AlN, pBN) under higher In evaporation conditions. Nanowire

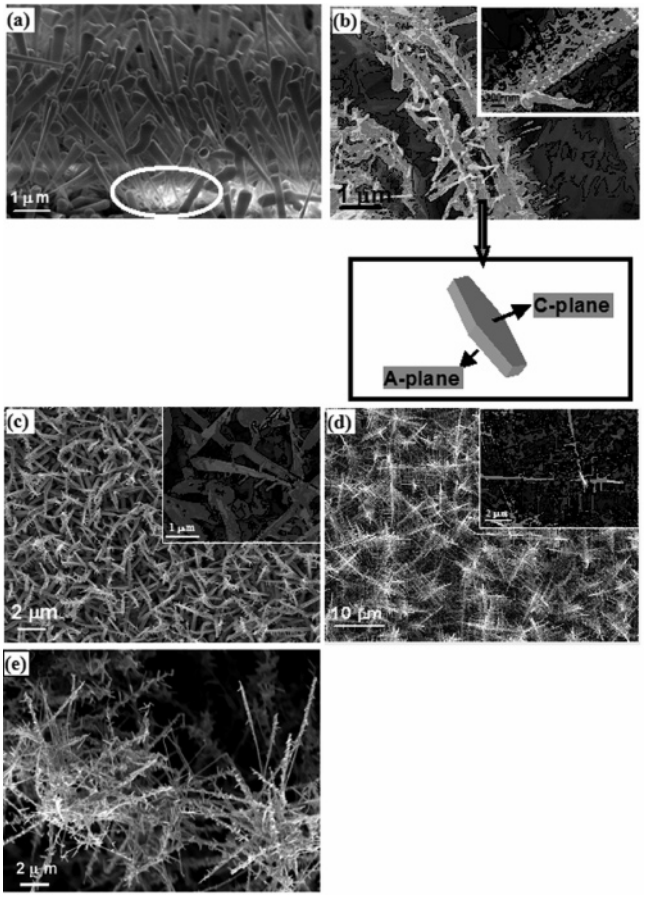

Figure 8. (a) Heteroepitaxially oriented InN nanowires synthesized on R-plane-oriented single-crystal sapphire substrates. The nanowires are tapered, and the diameter of the nanowires varies from 15 nm at the base to 100 nm at the top. The thin parts of the nanowires close to the substrate are highlighted in the figure. (b) High-magnification image and cartoon of the nanowires oriented perpendicular to the c plane of a GaN platelet. (c) Branched nanowires synthesized on an amorphous quartz substrate. (d) Multilevel branched nanowires synthesized on polycrystalline AlN substrates. The low-magnification image shows the branched nanowires. The high-magnification image in the inset shows the different levels of branching that occur. (e) Branched InN nanowires synthesized on pBN substrates.

branching occurred on all of the substrates (quartz, AlN and pBN), irrespective of the substrate material. See Figure 8c−e. The results in Figure 8d show the uniform formation of branched nanowires on an AlN substrate. Multilevel branching is shown clearly with the high-magnification image in the inset. The size of each branch is smaller than its stem that is expected with smaller In droplet condensation on a curved surface of the stem. These branched nanowires are always observed in the region of the substrate that is placed directly above the In source seeing an excess supply of In. A schematic representation of this region on the substrate is shown in Figure 1. Finally, electrical and optical characterization of the nanowires was performed to determine the band gap of InN and to explain the origin of the peak observed at 1.9 eV as well. To determine the electron energy spectrum of the InN nanowires, we performed photocurrent and scanning tunneling spectroscopy measurements.

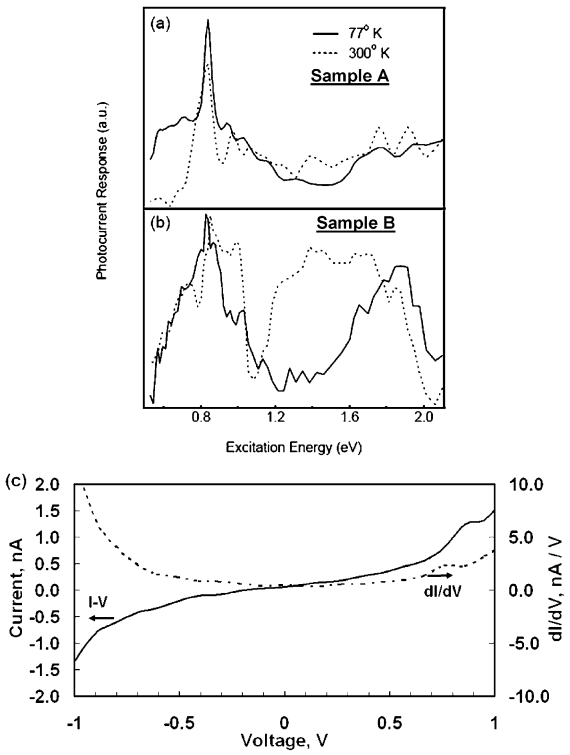

Figure 9. (a) Photoconductivity measurements of the synthesized InN nanowires bulk (sample A), showing the band gap to be 0.8 eV. (b) Photoconductivity measurements performed on a sample (sample B) having both InN and In_2O_3 phases, showing a peak at around 1.9 eV in addition to the peak at 0.8 eV. (c) STS (*I* vs *V* curve) of InN nanowires synthesized on HOPG substrates obtained under UHV conditions, clearly showing semiconductor behavior for InN. The curve showing the variation of d*I*/d*V* with voltage (*V*) is shown in the inset.

The photogenerated displacement current was measured across an MIS capacitor, in which the semiconductor electrode consists of InN nanowires grown on quartz or AlN substrates. Figure 9a shows the photocurrent as a function of excitation energy for a typical InN sample (sample A) measured at 77 and 300 K. A sharp peak in the photocurrent is observed for excitations near 0.8 eV. This is in agreement with photoluminescence measurements reported recently in which the band gap of InN nanowires was shown to be 0.8 eV. [9] Interestingly, the photocurrent measurements also reveal a possible explanation for previous experimental results suggesting that the InN band gap was 1.9 eV rather than 0.8 eV.[11] Figure 9b shows the photocurrent as a function of excitation energy for a second sample (sample B) synthesized on quartz substrate, in which peaks near 0.8 and 1.9 eV are observed. This sample (sample B) was synthesized specifically by using an as-received In source, without employing any acid-cleaning procedure that would have removed the native oxide layer. These experiments led to the formation of nanowires composed of both In_2O_3 and InN. XRD characterization (see supporting information) of this sample clearly revealed the presence of indium oxide (In_2O_3) in addition to InN. This implies that the peak at 1.9 eV is due to the presence of In_2O_3 in the sample. The energy of the peak near 1.9 eV increases with decreasing temperature, a behavior not observed in the 0.8 eV peak. This suggests that a high density of mid-gap states is associated with the 1.9 eV transition that freeze out at low temperatures. Such states could form at the nitride/oxide interface.

In addition, STS measurements were also performed on the synthesized InN nanowires to determine their band gap. A typical STS spectrum of the synthesized InN nanowires is presented in Figure 9c. These measurements were performed in a UHV environment (pressure $= 5 \times 10^{-10}$ Torr) using a platinum tip. Heteroepitaxially oriented InN nanowires synthesized on highly oriented pyrolytic graphite (HOPG) were used for these measurements. Excess indium at the tips of the nanowires was removed using sulfuric acid treatment, as mentioned above, before performing these measurements. Overall, the spectrum clearly shows the expected semiconducting behavior for InN. However, at low bias voltages a linear increase in current with bias voltage (ohmic behavior) was observed. Typically, doped or reconstructed semiconductor surfaces exhibit this behavior in the low bias region.[25] Extensive characterization of the synthesized nanowires (Figures 3 and 5) showed that they are composed of InN with excess indium at the tips of the nanowires. Also, as mentioned above, the excess indium at the tips of the nanowires was removed by acid-treatment before the STS measurements were performed. Doped semiconductors typically show huge increases in current under positive or negative bias, respectively, depending upon whether they are p-type or n-type.[26] Such a huge increase in current is not observed in our STS measurements on InN nanowires (Figure 9c). Also, the samples used for these measurements are not doped intentionally. However, the possibility of defect states (In or N related defect states) giving rise to this type of behavior exists. The other possible reason for the observed ohmic behavior is conduction through a reconstructed surface. Surface reconstruction is known to occur in III-nitride systems. This phenomenon was studied extensively and reported previously for GaN.[27−29] STS measurements on the Au-induced reconstruction of GaN surfaces, reported previously, showed behavior similar to that observed in our measurements.[29] Hence, the observed ohmic behavior in the low bias regime of InN might be due to either the presence of defect states or reconstruction of the surface.

In summary, the nucleation and early stages of growth mechanisms responsible for the 1D crystal growth in reactive vapor transport (or so-called self-catalysis) schemes have been studied, using InN nanowire synthesis as an example. The results indicate that initially the nucleation of InN crystals occurs on the substrate. This is followed by In droplet formation on these crystal nuclei because of selective wetting. The growth in one dimension occurs through In droplets via liquid-phase epitaxy with underlying InN crystals. This mechanism was employed for the synthesis of heteroepitaxially oriented InN nanowire arrays on R-plane oriented sapphire substrates. Also, the increased vapor transport of In onto growing nanowires resulted in tree-like nanowire formation with multilevel branching. In contrast, the direct nitridation of In droplets on amorphous quartz substrates led to the multiple nucleation and basal growth of InN nanowires

in the initial stages. The above mechanism of vapor phase epitaxy for InN crystals followed by liquid-phase epitaxy through In droplets on the crystals for 1D growth should hold true for all types of vapor transport schemes involving low-melting metals. Also, the observed phenomenon of multiple nucleation and growth of nanowires from low-melting metals could be accomplished even at room temperature by using activated nitrogen (using a radio frequency or electron cyclotron resonance plasma source) in the gas-phase instead of ammonia. The band gap of InN was measured to be 0.8 eV using photogenerated displacement current measurements. Similar measurements performed on a sample composed of both In_2O_3 and InN phases showed an additional peak at 1.9 eV, the value thought previously to be the band gap of InN. This peak at 1.9 eV can be attributed simply to the presence of In_2O_3 in the sample.

Acknowledgment. We thank Dr. W. Xu, University of Kentucky for help in performing TEM analysis of the nanowires. Partial financial support from the Kentucky Science and Engineering Foundation and NASA EPSCoR grants is gratefully acknowledged. Alan Chin is employed by Eloret Corporation, and his work at NASA Ames Research Center is supported by a subcontract from the University Affiliated Research Center (UARC), operated by University of California, Santa Cruz.

Supporting Information Available: XRD spectra of the synthesized InN nanowires, and mixed phases of In_2O_3 and InN are available. This material is available free of charge via the Internet at http://pubs.acs.org.

References

(1) Duan, X. F.; Lieber C. M. *J. Am. Chem. Soc.* **2000**, *122*, 128.
(2) Liang, C. H.; Chen, L. C.; Hwang, J. S.; Chen, K. H.; Hung, Y. T.; Chen, Y. F. *Appl. Phys. Lett.* **2002**, *81*, 22.
(3) Tang, T.; Han, S.; Jin, W.; Liu, X. L.; Li, C.; Zhang, D. H.; Zhou, C. W.; Chen, B.; Han, J.; Meyyappan, M. *J. Mater. Res.* **2004**, *19*, 423.
(4) Peng, H. Y.; Zhou, X. T.; Wang, N.; Zheng, Y. F.; Liao, L. S.; Shi, W. S.; Lee, C. S.; Lee, S. T. *Chem. Phys. Lett.* **2000**, *327*, 263.
(5) Sunkara, M. K.; Sharma, S.; Miranda, R.; Lian, G.; Dickey, E. C. *Appl. Phys. Lett.* **2001**, *79*, 1546.
(6) Chandrasekaran, H.; Sunkara, M. K. Growth of Gallium Nitride Textured Films and Nanowires on Polycrystalline Substrates at Sub-Atmospheric Pressures. MRS Symp. Proc., 2001; Vol. 693, p 159.
(7) Sharma, S.; Li, H.; Chandrasekaran, H.; Mani, R. C.; Sunkara, M. K. In *The Encyclopedia of Nanoscience and Nanotechnology*; Nalwa, H. S., Eds.; American Scientific Publishers: New York, 2003; and references therein.
(8) Sharma, S.; Sunkara, M. K. *J. Am. Chem. Soc.* **2002**, *124*, 12288.
(9) Graham, U. M.; Sharma, S.; Sunkara, M. K.; Davis, B. H. *Adv. Funct. Mater.* **2003**, *13*, 576.
(10) Johnson, M. C.; Lee, C. J.; Bourret-Courchesne, E. D.; Konsek, S. L.; Aloni, S.; Han, W. Q.; Zettl, A. *App. Phys. Lett.* **2004**, *85*, 5670.
(11) Zhang, J.; Zhang, L.; Peng, X.; Wang, X. *J. Mater. Chem.* **2002**, *12*, 802.
(12) Schwenzer, B.; Loeffler, L.; Seshadri, R.; Keller, S.; Lange, F. F.; DenBaars, S. P.; Mishra, U. K. *J. Mater. Chem.* **2004**, *14*, 637.
(13) Yin, L.-W.; Bando, Y.; Goldberg, D.; Li, M.-S. *Adv. Mater.* **2004**, *16*, 1833.
(14) Kuykendall, T.; Pauzauskie, P. J.; Zhang, Y. F.; Goldberger, J.; Sirbuly, D.; Denlinger, J.; Yang, P. D. *Nat. Mater.* **2004**, *3*, 524.
(15) Dick, K. A.; Deppert, K.; Larsson, M. W.; Martesson, T.; Seifert, W.; Wallenberg, L. R.; Samuelson, L. *Nat. Mater.* **2004**, *3*, 380.
(16) Matsuoka, T.; Okamoto, H.; Nakao, M.; Harima, H.; Kurimoto, E. *Appl. Phys. Lett.* **2002**, *81*, 1246.
(17) Vurgaftman, I.; Meyer, J. R.; Ram Mohan, L. R. *J. Appl. Phys.* **2001**, *89*, 5815.
(18) Yoshimoto, M.; Yamamoto, H.; Huang, W.; Harima, H.; Saraie, J.; Chayahara, A.; Horino, Y. *Appl. Phys. Lett.* **2003**, *83*, 3840.
(19) Mohite, A.; Chakraborty, S.; Gopinath, P.; Sumanasekera, G. U.; Alphenaar, B. W. *Appl. Phys. Lett.* **2005**, *86*, 061114.
(20) Davydov, V. Y.; Emtsev, V. V.; Goncharuk, I. N.; Smirnov, A. N.; Petrikov, V. D.; Mamutin, V. V.; Vekshin, V. A.; Ivanov, S. V. *Appl. Phys. Lett.* **1999**, *75*, 3297.
(21) Chen, Y. X.; Campbell, L. J.; Zhou, W. L. *J. Cryst. Growth* **2004**, *270*, 505.
(22) Toy, C.; Scott, W. D. *J. Mater. Sci.* **1997**, *32*, 3243.
(23) Li, H.; Chin, A.; Sunkara, M. K., 2005, manuscript in preparation.
(24) Jensen, L. E.; Bjork, M. T.; Jeppensen, S.; Persson, A. I.; Phlsson, B. J.; Samuelson, L. *Appl. Phys. Lett.* **2004**, *4*, 1961.
(25) Li, S. X.; Yu, K. M.; Jones, R. E.; Waluekiewicz, W.; Ager, J. W., III; Shan, W.; Haller, E. E.; Lu, H.; Schaff, W. A. *Phys. Rev. B* **2005**, *71*, 161201.
(26) Lin, H.-A.; Jaccodine, R.; Freund, M. S. *App. Phys. Lett.* **1998**, *72*, 1993.
(27) Feenstra, R. M.; Chen, H.; Ramachandran, V.; Smith, A. R.; Greve, D. W. *Appl. Surf. Sci.* **2000**, *166*, 165.
(28) Vezian, S.; Semond, F.; Massies, J.; Bullock, D. W.; Ding, Z.; Thibado, P. M. *Surf. Sci.* **2003**, *541*, 242.
(29) Maslova, N. S.; Panov, V. I.; Wu, K.; Xue, Q. Z.; Nagao, T.; Oreshkin, A. I. *JETP Lett.* **2003**, *78*, 578.

NL0505804